Photoacoustic Properties of Thin Film Zinc-Stannate

T. Ivetić[1a], M. V. Nikolić[2b], D. L. Young[3c], D. Vasiljević-Radović[4d], D. Urošević[5e]

[1]Institute of Technical Sciences of SASA, Knez Mihailova 35, 11000 Beograd, Serbia and Montenegro
[2]Center for Multidisciplinary Studies of the University of Belgrade, Kneza Višeslava 1, 11000 Beograd, Serbia and Montenegro
[3]National Renewable Energy Laboratory, Golden, Colorado 80401, USA
[4]Institute of Microelectronics and Single Crystals, Njegoševa 12, 11000 Beograd, Serbia and Montenegro
[5]Mathematical Institute, SASA, Knez Mihailova 35, 11000 Beograd, Serbia and Montenegro
[a]tamara@itn.sanu.ac.yu, [b]maria@mi.sanu.ac.yu, [c]david_young@nrel.gov, [d]dana@nanosys.ihtm.bg.ac.yu, [e]draganu@turing.mi.sanu.ac.yu

Abstract. Thin films of single-phase zinc-stannate (Zn_2SnO_4) were grown by rf magnetron sputtering onto glass substrates. Transmission in the visible range was measured allowing determination of the energy gap and thickness of analyzed thin film samples using interference fringes. The photoacoustic phase and amplitude spectra of all samples were measured as a function of the laser beam modulating frequency using a transmission detection configuration. Fitting of experimental data enabled calculation of thermal diffusivity, the coefficient of minority carrier diffusion, their mobility and lifetime.

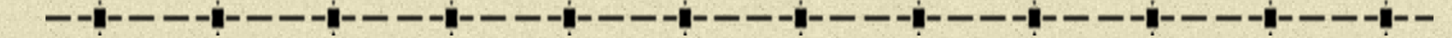

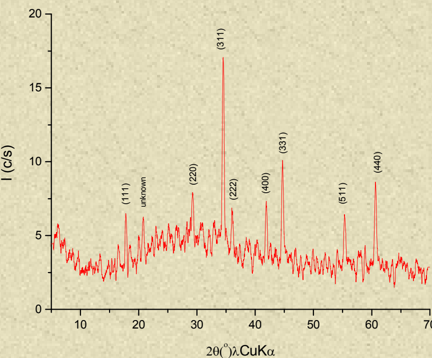

Fig. 1 XRD pattern of a typical Zn_2SnO_4 thin film sample after annealing

Transmission results of a typical Zn_2SnO_4 thin film sample after annealing are given in fig. 3. Film thickness and index of refraction were calculated using the interference fringes observed on fig. 3. The refractive index n_f of the thin film was first calculated using the following equation [1]:

$$n_f^2 = (n_a^2 + n_g^2)^2/2 + 2n_a n_g T_x + \left[\frac{(n_a^2 + n_g^2 + 4n_a n_g T_x}{4} - n_a^2 n_g^2\right]^{1/2} \quad (1)$$

where n_a is the refractive index of air, n_g is the refractive index of glass and n_f is the refractive index of the film,

$$T_x = \frac{T_{max} - T_{min}}{T_{max} T_{min}} \quad (2)$$

where T_{max} and T_{min} are the maximum and minimum of the transmittance versus the wavelength given in fig. 3.

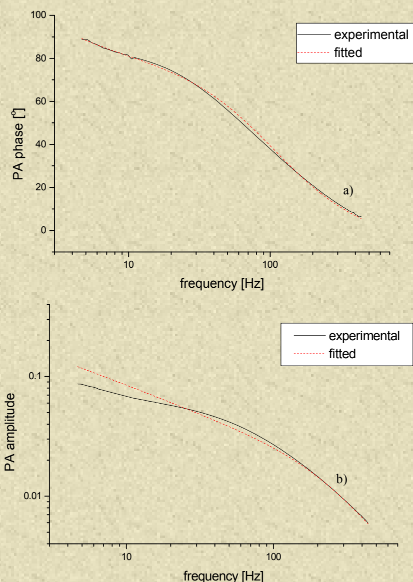

Fig. 4 Phase (a) and amplitude (b) experimental and theoretical diagrams for Zn_2SnO_4 thin film 600 nm thick

Results and Discussion

Fig. 1 shows the X-ray diffraction pattern of a typical Zn_2SnO_4 thin film sample after annealing. It was polycrystalline with peaks characteristic for spinel Zn_2SnO_4 and one small unknown peak at 4.321 A. The quality of the obtained sample surface is shown in fig. 2 giving typical AFM images of the analyzed Zn_2SnO_4 thin films. The images reveal "grains" with an average diameter of about 100nm.

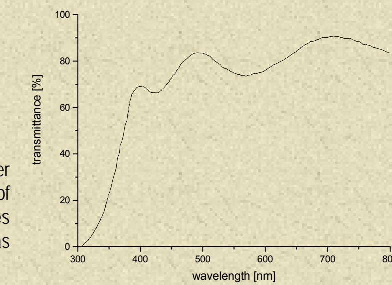

Fig. 3 Transmission vs. wavelength for a Zn_2O_4 thin film 600 nm thick

Fig. 4 shows the phase (a) and amplitude (b) of the photoacoustic signal vs. the modulating frequency for a typical Zn_2SnO_4 thin film sample 600 nm thick. A theoretical analysis of the experimental results of photoacoustic measurements was performed using the method described in detail in [3] based on the Rosencwaig-Gersho thermal piston model [4].

The experimental PA phase and amplitude diagrams were then fitted with the theoretically calculated PA signals for Zn_2SnO_4 thin films (fig. 4). A fitting procedure described in detail in [5] was then used to calculate thermal parameters of Zn_2SnO_4 thin films. The calculated values of the thermal parameters (D_T – the thermal diffusivity, τ - the excess carrier lifetime, D – the diffusion coefficient of the minority free carriers, α - the optical absorption coefficient, s_g and s_b are the front and rear surface recombination velocities) for two different thicknesses of Zn_2SnO_4 thin films are given in table 1. One can see that the values obtained for thermal diffusivity are very similar for both film thicknesses.

The mobility of minority free carriers for the analyzed Zn_2SnO_4 films were determined using the values calculated for the diffusion coefficient of the minority free carriers (D) and the following relation:

$$D = \frac{\mu T k}{e} \quad (4)$$

where k is the Boltzmann coefficient, e is the electron charge and T is the temperature, as the majority carrier effects are negligible for the cases when $n >> p$ or $p >> n$ according to the van Roosbroech ambipolar equation for the ambipolar diffusion coefficient [6]:

$$D^* = \frac{p + n}{p/D_n + n/D_p} \quad (5)$$

where p and n are the electron and hole concentration and D_n and D_p are the electron and hole diffusion coefficient, respectively. Thus, in this case $n >> p$ and $D^* = D_p = D$.

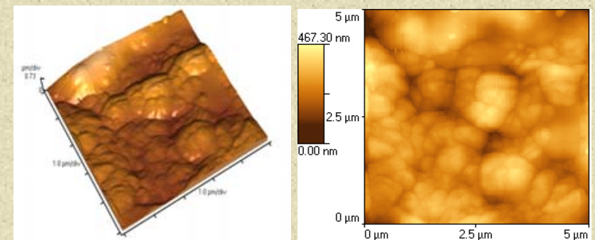

Fig. 2 AFM image of a Zn_2SnO_4 thin film 600 nm thick a) plan-view, b) 2D

The value obtained for the refractive index was n_f=1.94. The film thickness for each sample was calculated using the value obtained for the refractive index and the classical equation for interference fringes:

$$2dn_f = m\lambda \quad (3)$$

where d is the film thickness, m is the fringe order and λ is the wavelength. The values obtained were in the range of 316-600 nm (the sample given in fig. 3).

The direct band gap for each sample was calculated from the absorption edge. It read to be 0.325 nm for the sample 600 nm thick (fig. 3). The energy gap was calculated to be: E_g=1.24/0.325 = 3.81 eV. The values obtained for two film thicknesses are given in table 1. It is well known that the optical direct energy gap for Zn_2SnO_4 is about 3.35 eV. In our case the higher value of the energy gap is the consequence of a strong Burstein-Moss shift. The free carrier concentration of a sample with a film thickness of 643 nm was determined in [2] as $3.3 \cdot 10^{19}$ cm^3, so we expect this value to be higher for the thinner film with a higher energy gap.

Table 1 Calculated parameters for Zn_2SnO_4 thin films

Sample thickness	D_T (m²/s)	D (m²/s)	τ (s)	α (m^{-1})	s_g (m/s)	s_b (m/s)	μ (cm²/Vs)	E (eV)
600 nm	$0.1 \cdot 10^{-5}$	$0.50 \cdot 10^{-4}$	$4 \cdot 10^{-2}$	682	$0.2 \cdot 10^{-5}$	$0.5 \cdot 10^{-10}$	20	0.381
316 nm	$0.11 \cdot 10^{-5}$	$0.63 \cdot 10^{-4}$	$2 \cdot 10^{-2}$	11957	$0.5 \cdot 10^{-4}$	$0.2 \cdot 10^{-11}$	25	0.385

The values obtained for the minority carrier mobility for two film thicknesses are given in table 1. One can see that mobility was slightly higher for the thinner film. Both obtained values are in accordance with the ones calculated in [2] for different film thicknesses using the four-coefficient method for determining transport properties and the transport theory. Low mobility values and carrier concentrations are responsible for the high resistivities of Zn_2SnO_4 films. According to [2] incomplete crystallization of thin-film samples reflected in a larger full width at half maximum of XRD intensity peaks of thin films compared to the bulk sputter target could account for low mobility values. Minority carrier mobility is a parameter whose values could be useful for characterizing solar cell materials, as the minority carriers in absorber materials can be indicators of device performance.

References

1. S. Venkatachalam, D. Mangalaraj, Sa. K. Narayandass, K. Kim, J.Yi, Physica B: Condens. Matter, 358 (2005), 27-35
2. D. L. Young, H. Montinho, Y. Yan, T. J. Coutts, J. Appl. Phys. 92 (2002) 310-319
3. P. M. Nikolić, M. V. Nikolić, D. Luković, S. Savić, M. M. Ristić, Zeitschrift fur Metallkunde, 95 (2004), 147-150
4. A. Rosencwaig, A. Gersho, J. Appl. Phys. 47 (1976) 64-69
5. D. M. Todorović, P. M. Nikolić, Opt. Eng. (1997), 432-445
6. E. S. Yang, Fundamentals of semiconductor devices, Mc-Graw Hill, 1978

Acknowledgements

The authors would like to express their gratitude to Prof. P. M. Nikolić for many helpful conversations and S. Đurić for the X-ray measurements. This research was performed within projects 1832 and 6150 financed by the Ministry of Science and Environmental Protection of the Republic of Serbia.